The role of stratosphere-troposphere coupling in the occurrence of extreme winter cold spells over Northern Europe

Lorenzo Tomassini, Max Planck Institute for Meteorology, Bundesstrasse 53, D-20146, Hamburg, Germany (lorenzo.tomassini@zmaw.de).

Edwin P. Gerber, Center for Atmosphere Ocean Science, Courant Institute of Mathematical Sciences, New York University, New York, USA.

Mark P. Baldwin, College of Engineering, Mathematics and Physical Sciences, University of Exeter, Exeter, UK.

Felix Bunzel, Max Planck Institute for Meteorology, Bundesstrasse 53, D-20146, Hamburg, Germany.

Marco Giorgetta, Max Planck Institute for Meteorology, Bundesstrasse 53, D-20146, Hamburg, Germany.

Abstract. Extreme cold spells over Northern Europe during winter are examined in order to address the question to what degree and in which ways stratospheric dynamics may influence the state of the troposphere. The study is based on 500 years of a pre-industrial control simulation with a comprehensive global climate model which well resolves the stratosphere, the MPI Earth System Model. Geopotential height anomalies leading to cold air outbreaks leave imprints throughout the atmosphere including the middle and lower stratosphere. A significant connection between tropospheric winter cold spells over Northern Europe and erosion of the stratospheric polar vortex is detected up to 30hPa. In about 40 percent of the cases, the extreme cold spells are preceded by dynamical disturbances in the stratosphere. The strong warmings associated with the deceleration of the stratospheric jet cause the tropopause height to decrease over high latitudes. The compression of the tropospheric column below favors the development of high pressure anomalies and blocking signatures over polar regions. This in turn leads to the advection of cold air towards Northern Europe and the establishment of a negative annular mode pattern in the troposphere. Anomalies in the residual mean meridional circulation during the stratospheric weak vortex events contribute to the warming of the lower stratosphere, but are not key in the mechanism through which the stratosphere impacts the troposphere.

1. Introduction

Extended periods of cold temperatures in Europe during wintertime are generally of dynamic origin. High pressure anomalies over the Arctic or Siberia and low pressure over the European continent induce the advection of cold air from the north or the northeast towards lower latitudes. When this synoptic condition persists over several days, a cold spell occurs.

The described pattern of tropospheric pressure anomalies can sometimes be characterized by a negative phase of the North Atlantic Oscillation (NAO), as in the cold winter of 2010 (*Jung et al.* [2011]). In other instances, when the high pressure anomaly is centered more to the east over Scandinavia or Siberia, the dynamic situation is better described as an atmospheric block and does not well project on the NAO pattern. The anomalously cold winter of 2006 represents an example for such a case (*Croci-Maspoli and Davies* [2009]).

In both situations, the negative NAO phase and the high latitude blocking, the general westerly flow regime over the North Atlantic region is disturbed. Such a disturbance can sometimes extend through the whole troposphere and even into the stratosphere. For instance, during the cold winter of 2006, the northern hemispheric stratospheric vortex was particularly weak (*Scaife and Knight* [2008], *Jung et al.* [2010]).

The stratospheric polar vortex is a feature of the winter hemisphere climate. Although the stratospheric large-scale zonal flow is forced by differential diabatic heating, the winter stratosphere is not in radiative equilibrium (*Waugh and Polvani* [2010]). Vertically propagating planetary waves from the troposphere perturb the stratospheric circulation resulting in zonal winds that are weaker than predicted by radiative equilibrium (*Andrews et al.* [1987]). Such waves occasionally lead to rapid deceleration of the zonal flow and accompanying sudden warmings of the stratosphere (*Schoeberl* [1978]).

The traditional view on the coupling of the troposphere and the stratosphere is therefore centered on the impact of upward propagating tropospheric waves on the stratospheric dynamics. *Baldwin and Dunkerton* [1999] however showed by composite analysis of vertically resolved Northern Annular Mode (NAM) indices that stratospheric disturbances appear to propagate downward and become manifest in changes to the tropospheric circulation. In *Baldwin and Dunkerton* [2001] it is argued that weak stratospheric vortex regimes during northern winter cause statistically significant changes in the probabilities of cold air outbreaks across Europe, Asia, and North America.

However, since annular modes are calculated from geopotential height anomalies, they are partly an expression of temperature anomalies in underlying atmospheric layers. A vertically coherent structure in annular mode variability is therefore implicit in their definition. The central research question in this context thus concerns the issue to what extent and through which mechanisms a disturbance in the stratospheric polar vortex may propagate downwards and affect the tropospheric circulation.

The difficulty of this question consists in the fact that tropospheric disturbances may influence the flow regime in the troposphere as well as the dynamics of the stratosphere. *Polvani and Waugh* [2004] show that the initial stratospheric NAM anomalies in *Baldwin and Dunkerton* [2001] are themselves forced by wave breaking events originating from the troposphere. In *Gerber and Polvani* [2009], idealized model experiments show that topography can influence the position of the tropospheric jet as well as the variability in the stratospheric polar vortex. Thus, the correlation of the strength of stratospheric vortex with the position of the tropospheric jet does not necessarily imply that disturbances in the stratospheric circulation cause the tropospheric jet to shift.

A number of theories about the influence of the stratosphere on the troposphere have been proposed. *Hartley et al.* [1998] suggest that a redistribution of stratospheric potential vorticity induces perturbations in the upper troposphere (see also *Black* [2002] and *Black and McDaniel* [2004]). *Ambaum and Hoskins* [2002] stress the role of a change in tropopause height caused by stratospheric warmings (see also *Cai and Ren* [2007]). *Song and Robinson* [2004] describe mediating feedbacks to the stratospheric forcing by transient eddies (see also *Kushner and Polvani* [2004] and *Chen and Held* [2007]). Another line of reasoning concerns the modulation of reflected upward propagating tropospheric planetary waves by the strength of the wind shear in the lower stratosphere (*Perlwitz and Harnik* [2003]).

In the present paper we approach the question of possible impacts of stratospheric disturbances on the tropospheric circulation from the perspective of the troposphere. Strong and persistent surface temperature anomalies over Northern Europe are taken as a starting point of the investigation. This allows for studying cases where weak stratospheric polar vortex events and associated stratospheric warmings precede extreme negative temperature anomalies in the troposphere. In such instances atmospheric fields show distinct perturbations near the crucial region of the tropopause. By focusing on exceptionally strong signals, interactions of key dynamical features during stratosphere-troposphere coupling can be identified more clearly in the otherwise variable mid-latitude climate. The concentration on extreme events implies that long time series have to be considered.

Therefore the study centers on a long pre-industrial control integration with a coupled climate model, the MPI Earth System Model, that well resolves the stratosphere.

The article is structured as follows. In the second section the climate model and the simulation are described. The definition of cold spells and their tropospheric characteristics are contained in Section 3. Section 4 examines the question whether the anomalies in the stratosphere and the troposphere are related to each other in a significant way. In Section 5 a classification of cold spells is given based on the extent of the vertical coupling that can be observed during or before the event. Several diagnostics that illuminate the physical mechanisms acting during stratosphere-troposphere coupling are presented for cases of downward propagating disturbances in Section 6. Finally, a set of conclusions completes the paper.

2. Climate model and experiment

The Max Planck Institute Earth System Model (MPI-ESM) is based on the atmospheric general circulation model ECHAM6 (*Stevens et al.* [2012]), and an improved version of the Max Planck Institute Ocean Model MPI-OM (*Jungclaus et al.* [2012]). In the low resolution version (MPI-ESM-LR) used in this study, the atmospheric model utilizes a spectral transform dynamical core with triangular truncation at wavenumber 63, associated with a horizontal Gaussian grid with resolution of about 1.9 degrees. The vertical grid resolves the atmosphere in 47 levels up to 0.01 hPa. The model includes the Hines parameterization (*Hines* [1997a], *Hines* [1997b]) for the upward propagation of unresolved non-orographic gravity waves and their dissipation, providing tendencies in the horizontal winds. Its implementation follows *Manzini et al.* [2006]. The MPI-OM ocean model is a primitive equation model with a free surface and a mass flux boundary condition for salinity. A simple bottom boundary layer scheme is included as well as the standard set of subgrid-scale parameterizations. The model possesses a typical resolution of 1.5 degrees near the equator and 40 levels in the vertical.

The study focusses on 500 years of a MPI-ESM-LR pre-industrial control simulation with conditions of the year 1850, following the CMIP5 protocol (*Taylor et al.* [2012])). More details on the setup and performance of the simulation can be found in *Giorgetta et al.* [2012].

3. Winter cold spells over Northern Europe

For the definition of winter cold spells over Northern Europe we consider daily mean land temperature averaged over the geographic region of 0 East to 40 East and 48 North to 65 North (see the red box in the left panel of Figure 1). A cold spell is identified if the temperature drops below the 10 percent quantile of the climatological distribution for at least 15 consecutive days. In order to obtain a robust estimate of the 10 percent quantile, a 10 day moving window is used to calculate the daily climatological temperature distribution for each day in the year. Furthermore, we restrict our attention to cold spells that start or end in December, January, or February.

This definition of winter cold spells results in 41 of such cold air outbreaks over Northern Europe during the 500 years of the MPI-ESM pre-industrial control simulation. A composite of the 2-meter temperature anomaly for all winter cold spells is shown in Figure 1 (left panel). In the composite the temperature anomaly is rather confined over northeastern Europe. There is an extension towards Siberia but with an evidently flattening amplitude in eastern direction. In contrast, a distinct warm anomaly can be observed over Greenland, adjacent regions of the Arctic Ocean, and the most eastern part of Siberia.

This is in qualitative agreement with characteristics of recently observed European cold spells (e.g. *Croci-Maspoli and Davies* [2009]).

The corresponding composite of geopotential height anomalies at 500hPa (Figure 1, right panel) demonstrates the dynamic nature of the phenomenon. Low pressure slightly south of the region of cold air temperature, and a high pressure anomaly over the high latitudes north of Europe cause cold air from the northeast to advance towards the continent. The pattern is reminiscent of a negative phase of the North Atlantic Oscillation (NAO), but the NAO has its usual center of action over the North Atlantic Ocean. In the case of the cold spells the dominant geopotential height anomalies are located over land and north of Scandinavia. However, a trough of the low pressure area extends in westward direction towards the East Coast of the United States, an indication that in some cases a negative phase of the NAO is indeed responsible for the cold temperatures over Northern Europe.

A comparison of the simulated distribution of monthly mean winter land temperature anomalies over Northern Europe with observations (*Casty et al.* [2007]) shows that the pre-industrial control run well reproduces wintertime variability in this region (Figure 2). The lower tail of the distribution is particularly well captured by the model. Also stratospheric variability and the coupling of the stratosphere to the troposphere are satisfactorily represented by the model (*Charlton-Perez et al.* [2012]), as well as general Northern Hemispheric climate features (*Stevens et al.* [2012]).

The most prominent feature of the geopotential height anomaly composite in Figure 1 consists in the high latitude block. In some cold spell events it is situated right north of the continent, in some instances it is displaced slightly to the east or to the west.

We use a two-dimensional version of the Tibaldi-Molteni (*Tibaldi and Molteni* [1990]) blocking index as defined in *Scherrer et al.* [2006] in order to quantify the occurrence of high pressure blocks during the cold spells. The index assigns a 1 to days which show a blocking signature, and 0 to days without.

The left panel of Figure 3 shows the winter (NDJFM) blocking climatology of the pre-industrial control run, the right panel the composite of the blocking occurrence over the period of all cold spells subtracted from the climatology. In the composite the center of the block is located over the northern tip of Scandinavia stretching towards the east over the Barents Sea. This is in good agreement with studies of winter time blocking and their effect on the tropospheric climate based on reanalyses (e.g. *Trigo et al.* [2004]).

4. Significance of stratosphere-troposphere interaction

In the present paper we investigate the role of stratosphere-troposphere interactions in the development of Northern European winter cold spells. Since the seminal paper by *Baldwin and Dunkerton* [2001] the Northern Annual Mode (NAM) time series serves as most prominent stratosphere-troposphere coupling index (see also *Baldwin and Dunkerton* [1999]). In the following we use a NAM index based on daily zonally-averaged geopotential height as recommended in *Baldwin and Thompson* [2009] and employed also by *Gerber et al.* [2010]. The zonal-mean NAM is less prone to contamination by the Pacific/North American teleconnection (PNA) pattern, reflects well the daily evolution of stratosphere-troposphere coupling events, and can be computed consistently over the 500 years of the pre-industrial control simulation considered here.

In the stratosphere the zonal mean NAM index strongly correlates with zonal-mean wind anomalies between 40 North and 90 North (*Baldwin and Thompson* [2009]). Accordingly, for the present section, we define weak vortex events formally by requiring the centered NAM index to be below -1 times its standard deviation for at least 15 consecutive days. The persistence criterion is motivated by the interest in the relation of weak vortex events to cold spells. The NAM index time series is slightly smoothed using a 6-day Lanczos filter before the calculation of the weak vortex events in order not to let short nonfulfillments of the criterion have a major impact. Although in the troposphere the thus defined weak vortex events would more appropriately be called negative NAM events, for simplicity we will not make this terminological distinction.

Here we would like to assess if the connection between winter cold spells over Northern Europe and preceding weak vortex events is significant. This requires the definition of a significance measure and, as a prerequisite, a criterion that selects weak vortex events that are related to cold spells, at least in time.

Regarding the last point we define a weak vortex event to coincide with a cold spell if the weak vortex event starts before the end of the cold spell and ends no sooner than 40 days before the start of the cold spell. For the stratosphere higher than 100 hPa, “40 days” is replaced by “60 days” in the condition. This is motivated by *Baldwin and Dunkerton* [2001] where it is shown that the downward propagation of disturbances from the upper stratosphere to the lower troposphere exhibits a timescale of up to about 2 months.

In the following we assess the significance of the number of weak vortex events that coincide, in the above defined sense, with winter cold spells. To this end, the number of coincidences have to be related to the frequency of occurrence of weak vortex events as implied by their definition.

For each month in the year the frequency of occurrence of weak vortex events is first diagnosed from the pre-industrial control run. Then artificial start dates of weak vortex events are randomly sampled from all dates of each calender month in such a way that for each month in the year the number of such artificially generated weak vortex event start dates is the same as in the pre-industrial control run. Analogously, corresponding artificial end dates are determined in such a way that the mean and the standard deviation of the length of the artificially generated weak vortex events is the same as the mean and the standard deviation of the length of the actual weak vortex events in the pre-industrial control simulation.

Thus, the synthetically generated weak vortex events are equally frequent, but decorrelated in time from the simulated cold spells. This process is repeated 10'000 times. The distribution of coincidences of the artificial weak vortex events (Figure 4) can be compared to the actual number of coincidences in the pre-industrial control run (red lines in Figure 4). If the actual number of coincidences is at the upper end of the distribution of random coincidences, it is likely that there is a physical mechanism linking cold spells to weak vortex events in the pre-industrial control run. The grey shaded areas in Figure 4 indicate 2 standard deviations of the distributions.

Between 100 hPa and the surface, the consideration of a 40 days period and a 60 days period before the cold spells give qualitatively similar results, while higher up in the stratosphere the 40 days condition clearly leads to a less significant relation between weak vortex events and cold spells. Less significance in the upper stratosphere is not caused by lower numbers of actual coincidences in the control simulation, but by longer correlation times in the NAM index. The latter fact implies that the persistence criterion in the definition of weak vortex events is more readily met, which leads to an increase of the frequency of weak vortex events.

The significance of the relation of weak vortex events and cold spells that is evident in the troposphere and the lower stratosphere motivates to further investigate the physical mechanisms that vertically couple the stratosphere and the troposphere and relate surface cold spells to preceding stratospheric weak vortex events.

5. Dynamical classification of cold spells

As can be seen from Figure 5, the geopotential height anomalies over Northern Europe during the period of all cold spells persist up to the stratosphere and change their characteristics only at the 10hPa level. This is not per se particularly surprising as the geopotential height field tends to integrate temperature anomalies in the vertical.

The main point of interest in the present study therefore is the question whether there are cases of cold spells in which the origin of the dynamical disturbance can be traced back to the stratosphere. To examine this issue in more detail we categorize the 41 cold spells in the pre-industrial control run.

We call a cold spell stratospherically induced, or downward propagating, if we detect a coinciding weak vortex event at the 10hPa as well as at the 100hPa level. Here the definition of coinciding weak vortex events of Section 4 is adopted with two slight modifications. At 100hPa, we require the NAM index to stay below minus 0.8 times its standard deviation (instead of minus 1 times its standard deviation) to account for the higher variability at lower levels of the stratosphere. Moreover, the weak vortex events need to start strictly before the start of the cold spells.

Cold spells which meet this criterion at 100hPa but not at 10hPa are referred to as lower stratospheric cases. Finally we also need to formulate a formal definition of cold spells that are dynamically restricted to the troposphere. As can be seen from Figure 5, the dynamical characteristics of the northern European winter cold spells exhibit distinct regional features which do not always project equally well on the NAM pattern in the troposphere. Therefore, in order to detect atmospheric flow anomalies in the troposphere related to European cold spells, we introduce a more regional and flexible geopotential height based index than the NAM index.

This regional geopotential height index is defined by subtracting the maximum of the geopotential height anomaly over the area 30W to 90E and 65N to 80N from the minimum of the geopotential height anomaly over the area 0E to 40E and 45N to 55N. Applying this definition to the daily geopotential height anomaly field, and normalizing by the mean and standard deviation, results in a daily regional geopotential height index.

As can be seen from the geopotential height composites in Figure 5, negative anomalies are prevalent over Europe between 45N to 55N, and positive anomalies dominate north of the cold spell area in a band that covers 30W to 90E from the lower troposphere up to 30hPa. Using maxima and minima in the definition makes the index less dependent on a specific pre-selected pattern as in the case of the NAM. This flexibility is useful since the individual events have somewhat different synoptic features. As the regional north-south dipole of geopotential height anomalies, common to all cases, determines the specific atmospheric flow condition which leads to the cold spells, the index is suitable to describe the dynamical nature of the cold air outbreaks.

Cold spells that do not comply with the criteria of stratospherically induced or lower stratospheric events, but for which the regional geopotential height index stays below minus 0.8 times its standard deviation for at least 15 consecutive days at the 500hPa level within a period of 40 days before the start of the cold spell and the end of the cold spell, are termed tropospheric cases.

Of the 41 cold spells there are 17 stratospherically induced events, 8 lower stratospheric events, and 15 tropospheric cases. One cold spell does not fall in either of the categories. It is characterized by a strong and extended negative pressure anomaly over the European continent, Siberia, and large parts of the Arctic, and projects on a positive NAM index. Dynamically it is mainly confined to the troposphere, and we will not include this event in the following composite analysis.

In order to discuss the dynamical signatures of the three classes we introduce two more indices similar in spirit to the regional geopotential height index. A regional wind index is defined as the mean of the zonal wind anomaly over Northern Europe where the cold spells occur (0E to 40E and 48N to 65N). In the troposphere it is indicative of the easterly flow which leads to the cold air outbreaks, while in the stratosphere it characterizes the strength of the polar vortex. Analogously, a regional temperature index is explained as the mean of the temperature anomalies over the area 0E to 40E and 55N to 65N. Both indices are normalized by their respective means and standard deviations. The temperature index is confined to 55N (instead of 48N) since at higher levels of the atmosphere, temperature anomalies that are associated with dynamical disturbances in the stratosphere tend to weaken towards lower latitudes (*Schoeberl* [1978]).

Figure 6 shows the time development of the different indices for the three cold spell classes. Day 0 in the stratospherically induced case is defined as the start of the weak vortex event at the 10hPa level. For the lower stratospheric case, day 0 in the composite is determined by the start of the weak vortex event at the 100hPa level. In the tropospheric case day 0 corresponds to the start of the dynamical disturbance as defined by the regional geopotential height index at 500hPa.

The panels in Figure 6 include stippled areas which indicate a measure of significance with respect to natural variability. For each index and level of the atmosphere, N arbitrary winter days are sampled, where N is the number of events that enter the respective composite. The mean is calculated over these N days. This procedure is then repeated 10'000 times. The stippled regions indicate the areas where the composite exceeds 2 standard deviations of the distributions of these mean values.

One can see that the tropospheric events are indeed mainly restricted to the troposphere. During the cold spell one can identify a signal in the geopotential height index (and, in accordance, in the zonal wind and the temperature index) also in the stratosphere, but this is rather a consequence of the temperature anomaly at lower levels than the cause of the cold spell.

Also for the lower stratospheric cases there are indications that the dynamical disturbances originate in the troposphere. In all indices there are, to some degree, signals in the troposphere before day 0 of the composite, and effects in the stratosphere occur instantaneously or later in time.

The situation is different, although not completely unambiguous, in the case of the stratospherically induced events. In the NAM index the signal in the stratosphere shows up prior to the disturbance in the troposphere. It is evident rather instantaneously throughout the stratosphere, but the persistence of the anomalies is larger in the lower stratosphere. However, in the regional geopotential height index and the regional wind index, anomalies are present in the troposphere before the main development of the events in the stratosphere. The tropospheric disturbances could have been, at least partially, the cause of increased wave breaking and deceleration of the vortex in the stratosphere (*Cohen et al.* [2007]). *Black and McDaniel* [2004] give evidence that the possibility for stratosphere-troposphere interactions depends on the preexisting state of the troposphere. A particularly clear downward propagating signal seems to be present in the regional mid-latitudinal temperature index. In the next section we focus on the stratospherically induced cold spell events and further investigate the physical mechanisms of the stratosphere-troposphere coupling.

6. Mechanisms of stratosphere-troposphere coupling

When the composite of temperature anomalies over Northern Europe (first row of Figure 7, left panel, same as in Figure 6) is compared to the temperature anomalies calculated over the polar area of 0E to 40E and 70N to 90N (Figure 7, first row, right panel), it is apparent that over the polar region the positive temperature anomalies become effective immediately after the start of the vortex disturbance across the whole stratosphere. As a consequence, the tropopause is continuously lowered (Figure 7, fourth row). Here again an area average is taken over the region 0E to 40E and 70N to 90N for the right panel, and 0E to 40E and 55N to 65N for the left panel.

With some time delay negative temperature anomalies, indicative of changes in the tropospheric circulation, develop over Northern Europe, and negative potential vorticity anomalies accumulate in the lower stratosphere and penetrate through the tropopause, mostly over the polar region (Figure 7, third row).

Here we use the thermal definition of the tropopause according to which the tropopause is identified as the lowest altitude where the temperature lapse rate is smaller than 2 Kelvin per km, provided that the average lapse rate from this level to any point within 2 km above also features a lapse rate smaller than 2 Kelvin per km (see *Gettelman et al.* [2011] for a discussion of different tropopause definitions). The change in the tropopause height during weak vortex events is an immediate consequence of the strong warming of the lower stratosphere, and is further amplified by dynamical feedbacks which cause a cooling in the troposphere.

An impact of the strength of the polar vortex on the tropospheric circulation is established in *Ambaum and Hoskins* [2002] by exploring the effect of potential vorticity anomalies in the stratosphere on the tropopause height, and the consequence of changed tropopause height for surface pressure over the North Pole. The theory is developed in the context of a quasigeostrophic model from which a potential vorticity equation is derived. Here again, negative potential vorticity anomalies in the stratosphere result in a lowered tropopause, a compressed tropospheric column below, and consequently a reduced relative vorticity over the polar cap associated with a high pressure signal. Similar ideas were put forward in *Hartley et al.* [1998] and *Black* [2002], and a general discussion of what factors control the tropopause height is contained in *Schneider* [2007]. *Black and McDaniel* [2004] point out that the potential vorticity anomalies need to descend to sufficiently low altitudes within the stratosphere in order to have an effect on the troposphere.

Figure 8 presents the time development of potential vorticity anomalies before and during the downward propagating cold spells, significant regions are stippled. The left column contains a mean over days 30 to 15 before the start of the cold spells, the mid column a mean over day 15 to day 1 before, and the right column a mean over day 1 to day 15 of the cold spells. One can observe that negative potential vorticity anomalies develop at 50hPa (first row) over polar regions before the cold spells. They intensify during the 15 days before the cold spells, and become evident in the lower stratosphere as well. In the troposphere, at the 500hPa geopotential height level (fourth row), the anomalies are most pronounced during the cold spells.

Polvani and Kushner [2002] report, based on simulations with a simplified general circulation model, a poleward shift of the tropospheric jet when the stratosphere is cooled and thus the stratospheric vortex strengthened. Similarly, *Williams* [2006] describes how increased temperatures in the stratosphere and an associated lower tropopause height shift the tropospheric jet equatorwards in idealized model simulations.

This mechanism implies a certain time delay and potentially an elongation of time scales. *Gerber and Vallis* [2007] show that in idealized model experiments the interaction between synoptic eddies retard the motion of the jet, slowing its meridional variation and thereby extending the persistence of annular mode anomalies in the troposphere. The negative zonal-mean zonal wind anomalies are evident in the stratosphere in the days 45 to 30 before the start of the cold spells (Figure 9 upper row, right panel). During day 30 to day 1 before the cold spells (lower row, left and mid panel), the poleward flank of the tropospheric jet over the North Atlantic gradually weakens, while the equatorward side strengthens. The negative zonal wind anomalies of the stratosphere extend downward into the troposphere over the region of the occurrence of the cold spells. The strengthening of the zonal wind at the southern side of the area of surface temperature anomalies is consistent with the geopotential height anomaly pattern (Figure 5).

Thus, a dynamical feedback can be identified. The lowering of the tropopause caused by the stratospheric warming over the polar cap produces a tropospheric high pressure anomaly over the polar region which leads to the advection of cold air towards Northern Europe. The resulting cold air outbreak induces negative geopotential height anomalies over the continent which amplifies the negative NAM signature. At the southern flank of the cold spell area the meridional pressure gradient and consequently the zonal flow are enhanced. In accordance with *Charlton et al.* [2005], the impact of the stratosphere on the troposphere is therefore mediated through synoptic-scale systems and can not be understood merely as a large-scale adjustment of the troposphere to stratospheric potential vorticity anomalies.

Near the extratropical tropopause and lower stratosphere, the stratospheric residual circulation provides adiabatic warming which contributes to the lowering of the extratropical tropopause (*Son et al.* [2007], *Birner* [2010]). In the second row of Figure 7 a composite of the Eliassen-Palm flux divergence (left panel) and the residual circulation mass stream function (right panel) for the downward propagating cold spells are shown. Quantities are averaged over the latitudes 65N to 75N, the qualitative picture does however not depend on the exact region considered. Increased Eliassen-Palm flux divergence during the early stage of the stratospheric disturbance confirms the crucial role of wave breaking in the development of stratospheric weak vortex events and associated warmings (*Schoeberl* [1978]). Significant anomalies in the strength of the residual circulation occur mainly at the beginning of the stratospheric vortex disturbance. This suggests that the residual mean meriodional circulation does not directly play a decisive role in the mechanism through which the stratosphere impacts the troposphere. Rather, in accordance with *Cai and Ren* [2007], the apparent downward propagation of stratospheric disturbances into the troposphere is a consequence of the dynamic response to heating and cooling anomalies.

7. Conclusions

Extreme winter cold spells over Northern Europe with a return period of about 12 years are investigated in a long pre-industrial control simulation using the MPI Earth System Model. A significant relation between such cold air outbreaks and preceding circulation anomalies in the stratosphere up to at least 50hPa can be detected. 17 out of 41 cold spells occur in association with a downward propagating dynamical disturbance which originates in the stratosphere. However, also in these cases preexisting geopotential height anomalies reminiscent of a negative annular mode pattern are present in the troposphere.

A composite analysis of the downward propagating cases reveals the important role of wave breaking in the development of stratospheric vortex anomalies. Vertically propagating planetary waves disturb the stratospheric circulation and transport heat and momentum from mid-latitudes into the polar region, causing strong stratospheric warmings. Immediate temperature increases can be observed over the polar cap, while over the mid-latitudes the temperature signal exhibits a downward propagating structure representing the dynamical evolution of the stratospheric vortex disturbance. In the lower stratosphere and near the tropopause, the temperature anomalies persist due to the relatively low efficiency of radiative cooling at these height levels (*Kiehl and Solomon* [1986]). Anomalies in the residual mean meridional circulation partly contribute to the adiabatic warming in the lower stratosphere, but the anomaly in the residual circulation mass stream function is mainly restricted to the period of the strongest dynamical disturbance in the stratosphere.

As a consequence of the warming in the lower stratosphere, the tropopause height is lowered which leads to a compression of the tropospheric column below and a high pressure signature over the polar region in the troposphere. Zonal wind anomalies are thus transferred from the stratosphere to the troposphere, and the advection of cold air from the northeast towards Northern Europe further reinforces the negative NAM pattern in the troposphere.

The impact of the stratosphere on the troposphere can thus be understood as dynamical response to heating anomalies rather than the effect of stratospheric momentum forcing on the meridional circulation as expressed in the so-called "principle of downward control" (*Haynes et al.* [1991]), originally formulated in a zonally symmetric context. The dynamical feedback amplifies the effect of the lower stratospheric perturbation in the troposphere.

Acknowledgments. Useful comments by Elisa Manzini greatly helped to guide the analysis. Support by James Anstey, who provided the code for the blocking index computation, as well as the Max Planck Society for the Advancement of Science, is gratefully acknowledged. We thank Hauke Schmidt for a careful reading of the manuscript, and the German Climate Computing Center (DKRZ) for the provision of the simulation. The work was partially funded by the European Commission's 7th Framework Programme, under GA 226520 for the COMBINE project.

References

Ambaum, M. H. P., and B. J. Hoskins (2002), The NAO troposphere-stratosphere connection, *J. Climate*, *15*, 1969–1978.

Andrews, D. G., J. R. Holton, and C. B. Leovy (1987), *Middle atmosphere dynamics*, 489 pp., Academic Press, San Diego.

Baldwin, M. P., and T. J. Dunkerton (1999), Propoagation of the Arctic Oscillation from the stratosphere to the troposphere, *J. Geophys. Res.*, *104*, 30,937–30,946.

Baldwin, M. P., and T. J. Dunkerton (2001), Stratospheric harbingers of anomalous weather regimes, *Science*, *294*, 581–584.

Baldwin, M. P., and D. W. J. Thompson (2009), A critical comparison of stratosphere-troposphere coupling indices, *Q. J. R. Meteorol. Soc.*, *135*, 1661–1672.

Birner, T. (2010), Residual circulation and tropopause structure, *J. Atmos. Sci.*, *67*, 2582–2600.

Black, R. X. (2002), Stratospheric forcing of surface climate in the Arctic oscillation, *J. Climate*, *15*, 268–277.

Black, R. X., and B. A. McDaniel (2004), Diagnostic case studies of the Northern Annular Mode, *J. Climate*, *17*, 3990–4004.

Cai, M., and R.-C. Ren (2007), Meridional and downward propagation of atmospheric circulation anomalies. Part I: Northern hemisphere cold season variability, *J. Atmos. Sci.*, *64*, 1880–1901.

Casty, C., C. C. Raible, T. F. Stocker, J. Luterbacher, and H. Wanner (2007), A European pattern climatology 1766-2000, *Climate Dynamics*, doi:10.1007/s00382-007-0257-6.

Charlton, A. J., A. O'Neill, P. Berrisford, and W. A. Lahoz (2005), Can the dynamical impact of the stratosphere on the troposphere be described by large-scale adjustment of the stratospheric PV distribution, *Q. J. R. Meteorol. Soc.*, *131*, 525–543.

Charlton-Perez, A. J., et al. (2012), Mean climate and variability of the stratosphere in the CMIP5 models, in preparation.

Chen, G., and I. M. Held (2007), Phase speed spectra and the recent poleward shift of Southern Hemisphere surface westerlies, *Geophys. Res. Lett.*, *34*, doi: 10.1029/2007GL031200.

Cohen, J., M. Barlow, P. J. Kushner, and K. Saito (2007), Stratosphere-troposphere coupling and links with Eurasia land surface variability, *J. Climate*, *20*, 5335–5343.

Croci-Maspoli, M., and H. C. Davies (2009), Key daynamical features of the 2005/2006 European winter, *Mon. Wea. Rev.*, *137*, 664–678.

Gerber, E. P., and L. Polvani (2009), Stratosphere-troposphere coupling in a relatively simple AGCM: The importance of stratospheric variability, *J. Climate*, *22*, 1920–1933.

Gerber, E. P., and G. K. Vallis (2007), Eddy-zonal flow interactions and the persistence of the zonal index, *J. Atmos. Sci.*, *64*, 3296–3311.

Gerber, E. P., et al. (2010), Stratosphere-troposphere coupling and annular mode variability in chemestry-climate models, *J. Geophys. Res.*, *115*, doi:10.1029/2009JD013770.

Gettelman, A., P. Hoor, L. L. Pan, W. J. Randel, M. I. Hegglin, and T. Birner (2011), The extratropical upper troposphere and lower stratosphere, *Rev. Geophys.*, *49*, doi: 10.1029/2011RG000355.

Giorgetta et al., M. (2012), Climate variability and climate change in the MPI-ESM CMIP5 simulations, in preparation.

Hartley, D. E., J. T. Villarin, R. X. Black, and C. A. Davis (1998), A new perspective on the dynamical link between the stratosphere and troposphere, *Nature*, *391*, 471–474.

Haynes, P. H., C. J. Marks, M. E. McIntyre, T. G. Shepherd, and K. P. Shine (1991), On the "downward control" of extratropical diabatic circulations by eddy-induced mean zonal forces, *J. Atmos. Sci.*, *48*, 651–678.

Hines, C. O. (1997a), Doppler spread parameterization of gravity wave momentum deposition in the middle atmosphere. Part I: Basic formulation, *J. Atmos. Solar Terr. Phys.*, *59*, 371–386.

Hines, C. O. (1997b), Doppler spread parameterization of gravity wave momentum deposition in the middle atmosphere. Part II: Broad and quasimonochromatic spectra and implementation, *J. Atmos. Solar Terr. Phys.*, *59*, 387–400.

Jung, T., T. N. Palmer, M. J. Rodwell, and S. Serrar (2010), Understanding the anomalously cold European winter of 2005/06 using relaxation experiments, *Mon. Wea. Rev.*, *138*, 3157–3174.

Jung, T., F. Vitart, L. Ferranti, and J.-J. Morcrette (2011), Origin and predictability of the extreme negativ NAO winter of 2009/10, *Geophys. Res. Lett.*, *38*, doi: 10.1029/2011GL046786.

Jungclaus et al., J. (2012), Characterictics of the ocean simulations in the MPI Earth System Model, in preparation.

Kiehl, J. T., and S. Solomon (1986), On radiative balance of the stratosphere, *J. Atmos. Sci.*, *43*, 1525–1534.

Kushner, P. J., and L. Polvani (2004), Stratosphere-troposphere coupling in a relatively simple AGCM: The role of eddies, *J. Climate*, *17*, 629–639.

Manzini, E., M. A. Giorgetta, M. Esch, L. Kornblueh, and E. Roeckner (2006), The influence of sea surface temperatures on the northern winter stratosphere: ensemble simulations with the MAECHAM5 model, *J. Climate*, *19*, 3863–3881.

Perlwitz, J., and N. Harnik (2003), Observational evidence of a stratospheric influence on the troposphere by planetary wave reflection, *J. Climate*, *16*, 3011–3026.

Polvani, L., and P. J. Kushner (2002), Tropospheric response to stratospheric perturbations in a relatively simple general circulation model, *Geophys. Res. Lett.*, *29*, doi: 10.1029/2001GL014284.

Polvani, L. M., and D. W. Waugh (2004), Upward wave activity flux as a precursor to extreme stratospheric events and subsequent anomalous surface weather regimes, *J. Climate*, *17*, 3548–3554.

Scaife, A. A., and J. R. Knight (2008), Ensemble simulations of the cold European winter of 2005-2006, *Q. J. R. Meteorol. Soc.*, *134*, 1647–1659.

Scherrer, S. C., M. Croci-Maspoli, C. Schwierz, and C. Appenzeller (2006), Two-dimensional indices of atmospheric blocking and their statistical relationship with winter climate patterns in the Euro-Atlantic region, *Int. J. Climatol.*, *26*, 233–249.

Schneider, T. (2007), The thermal stratification of the extratropical troposphere, in *The global circulation of the atmosphere*, edited by T. Schneider and A. H. Sobel, pp. 47–77, Princeton University Press, Princeton.

Schoeberl, M. R. (1978), Stratospheric warmings: Observations and theory, *Rev. Geophys.*, *16*, 521–538.

Son, S.-W., S. Lee, and S. B. Feldstein (2007), Intraseasonal variability of the zonal-mean extratropical tropopause height, *J. Atmos. Sci.*, *64*, 608–620.

Song, Y., and W. A. Robinson (2004), Dynamical mechanisms for stratospheric influences on the troposphere, *J. Atmos. Sci.*, *61*, 1711–1725.

Stevens, B., et al. (2012), The atmospheric component of the MPI Earth System Model: ECHAM6, in preparation.

Taylor, K. E., R. J. Stouffer, and G. A. Meehl (2012), An overview of CMIP5 and the experiment design, *BAMS*, doi:10.1175/BAMS-D-11-00094.1.

Tibaldi, S., and F. Molteni (1990), On the operational predictability of blocking, *Tellus*, *42A*, 343–365.

Trigo, R. M., I. F. Trigo, C. C. DaCamara, and T. J. Osborn (2004), Climate impact of the European winter blocking epsiodes from the NCEP/NCAR reanalyses, *Climate Dynamics*, *23*, doi:10.1007/s00382-004-0410-4.

Waugh, D. W., and L. Polvani (2010), Stratospheric polar vortices, in *The stratosphere: Dynamics, transport, and chemistry*, edited by L. M. Polvani, A. H. Sobel, and D. W. Waugh, pp. 43–57, AGU Geophys. Monogr. Ser., Washington, D. C., doi: 10.1029/2009GM000887.

Williams, G. P. (2006), Circulation sensitivity to tropopause height, *J. Atmos. Sci.*, *63*, 1954–1961.

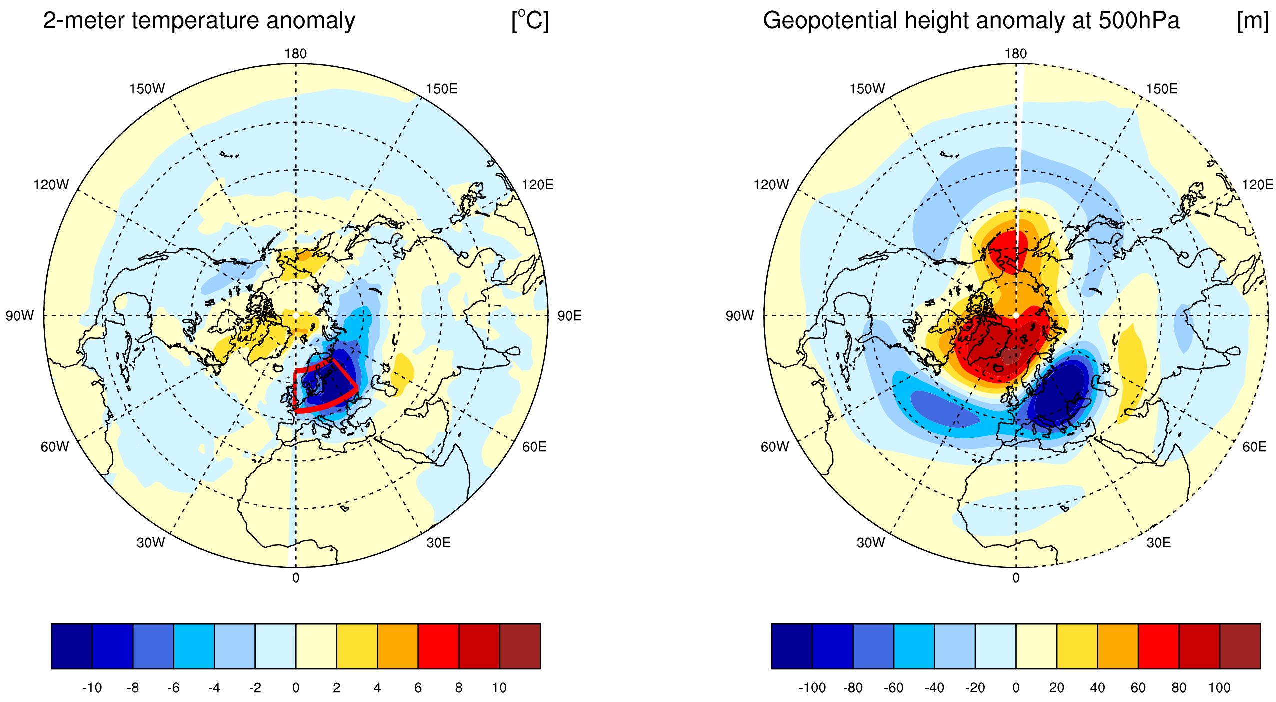

Figure 1. Left panel: composite of the 2-meter temperature anomaly for all winter cold spells. Right panel: corresponding composite of geopotential height anomalies at 500hPa.

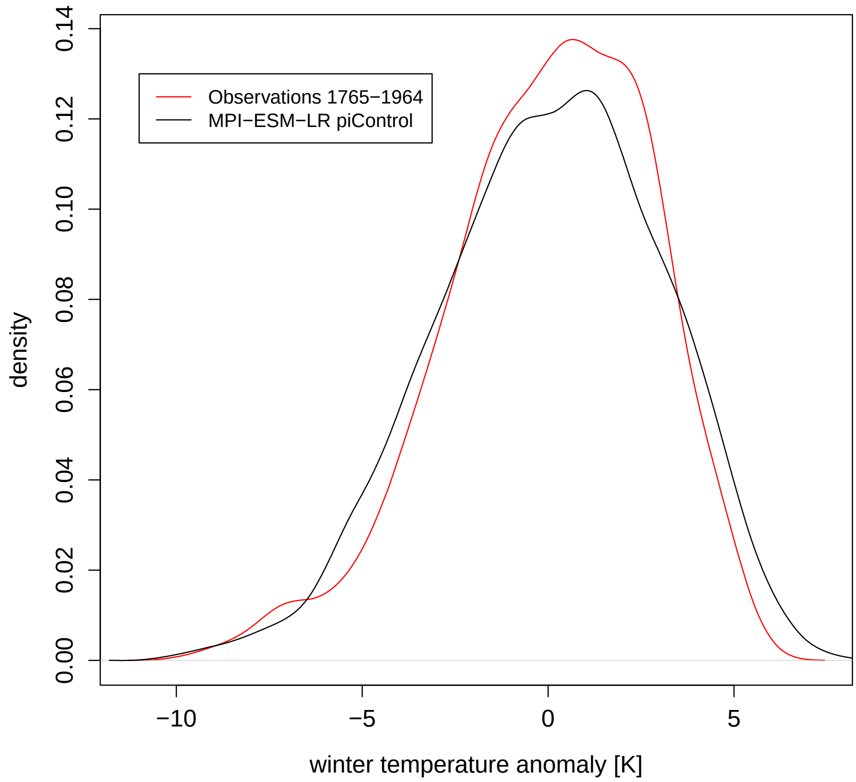

Figure 2. Distribution of monthly winter temperature anomalies over the land area of 48 North to 65 North and 0 East to 40 East based on observations for the period 1765 to 1964 (*Casty et al.* [2007]) and 500 years of the MPI-ESM-LR pre-industrial control simulation.

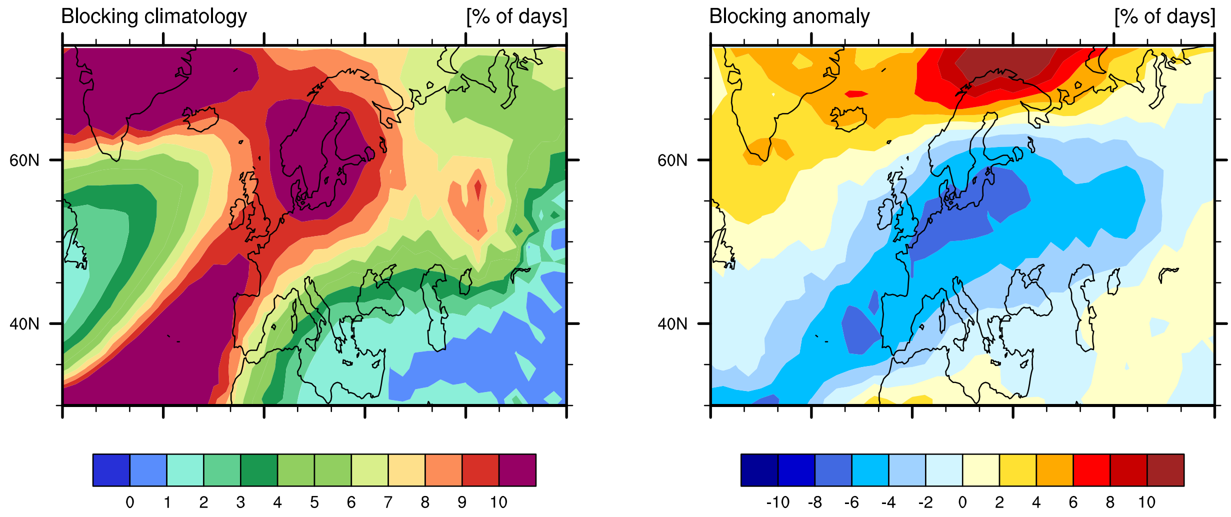

Figure 3. Left panel: winter (NDJFM) blocking climatology of the MPI-ESM pre-industrial control run. Right panel: composite of the blocking occurrence anomalies over the period of all cold spells. Blocking occurrence is measured in percentage of days with blocking signature.

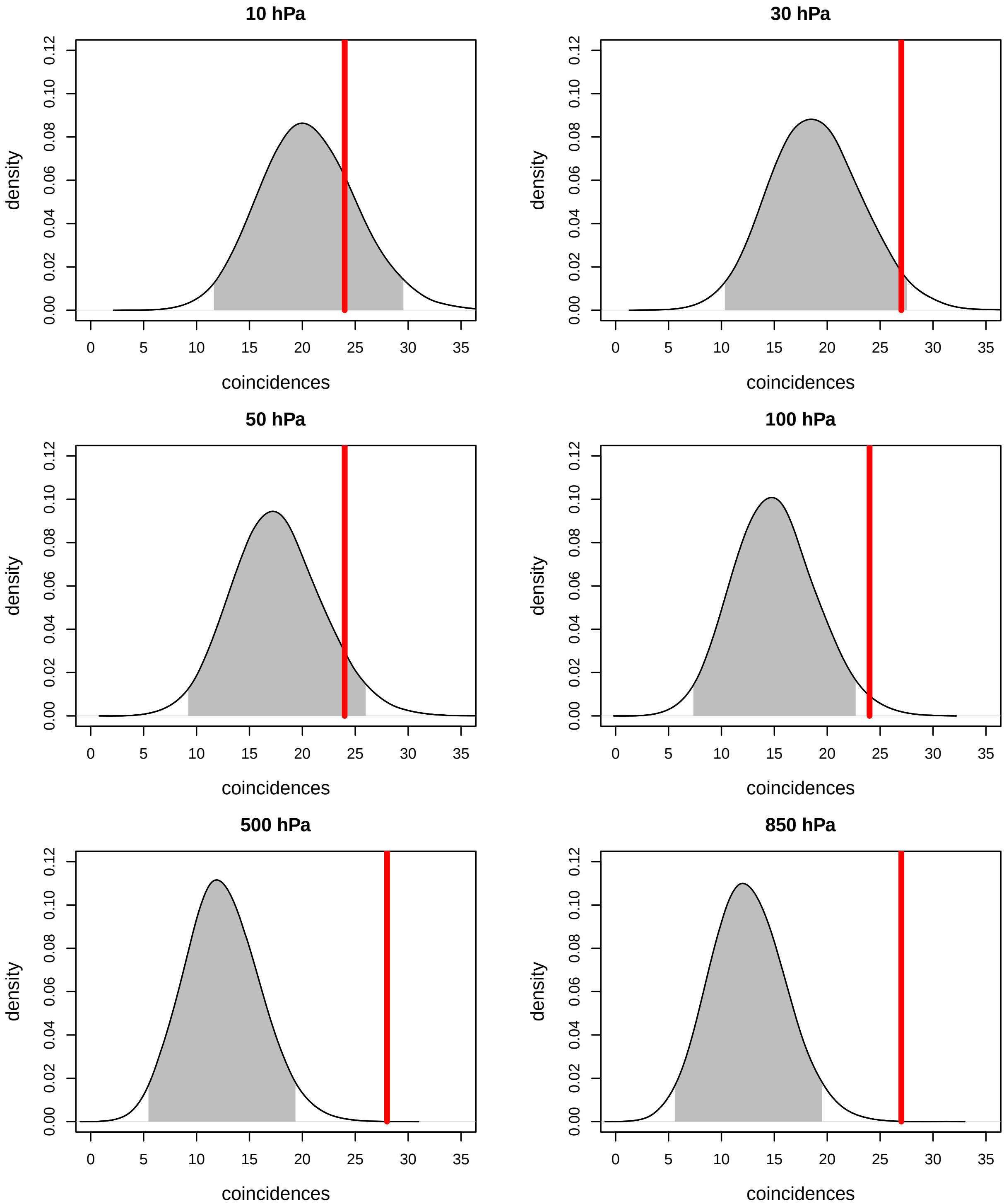

Figure 4. Distribution of coincidences of artificially sampled weak vortex events with the winter cold spells at different pressure levels. The actual number of coincidences in the pre-industrial control run are indicated by red lines. Grey shaded areas indicate 2 standard deviations of the distributions.

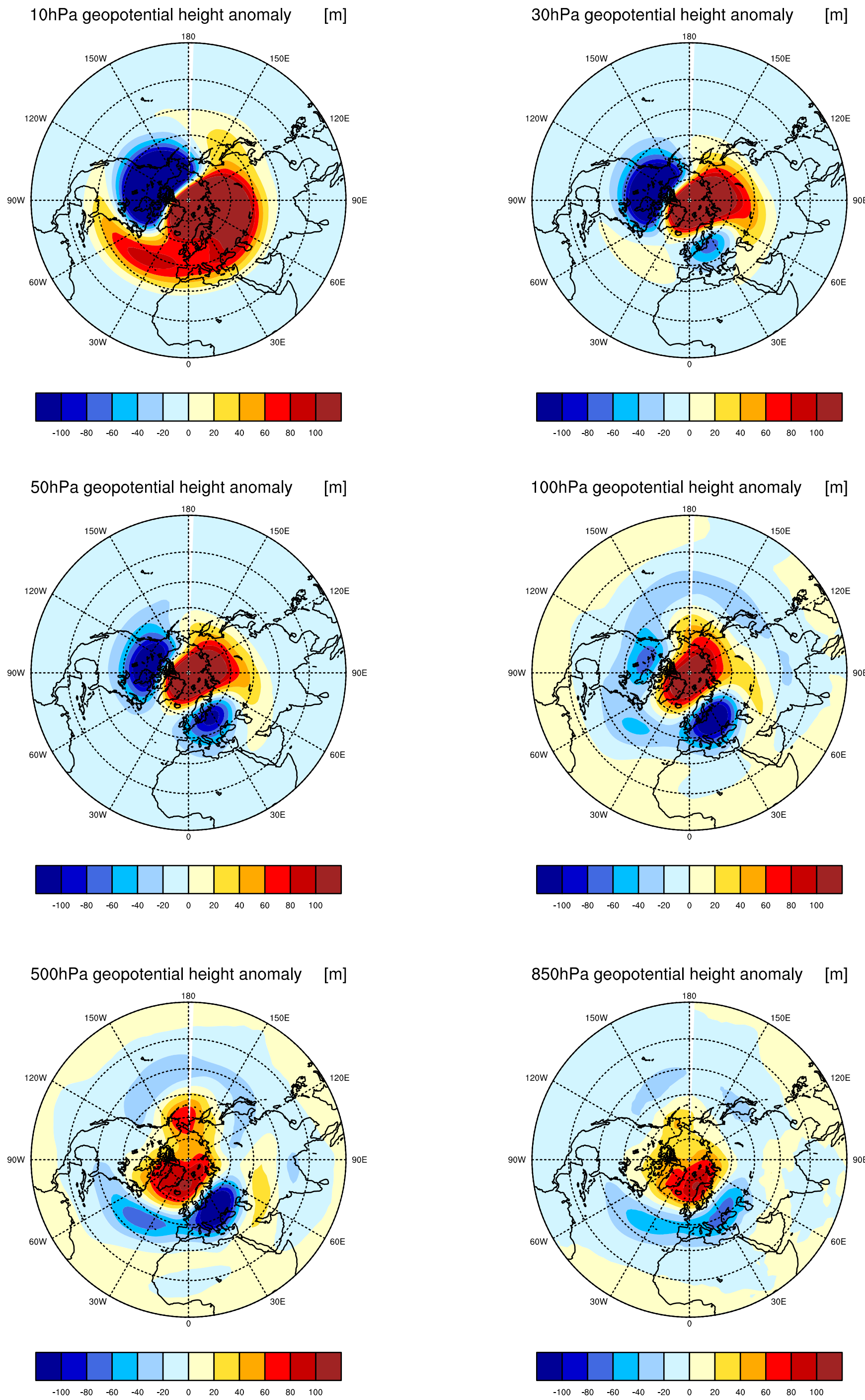

Figure 5. Geopotential height anomalies over the Northern Hemisphere during the period of all cold spells at different pressure levels.

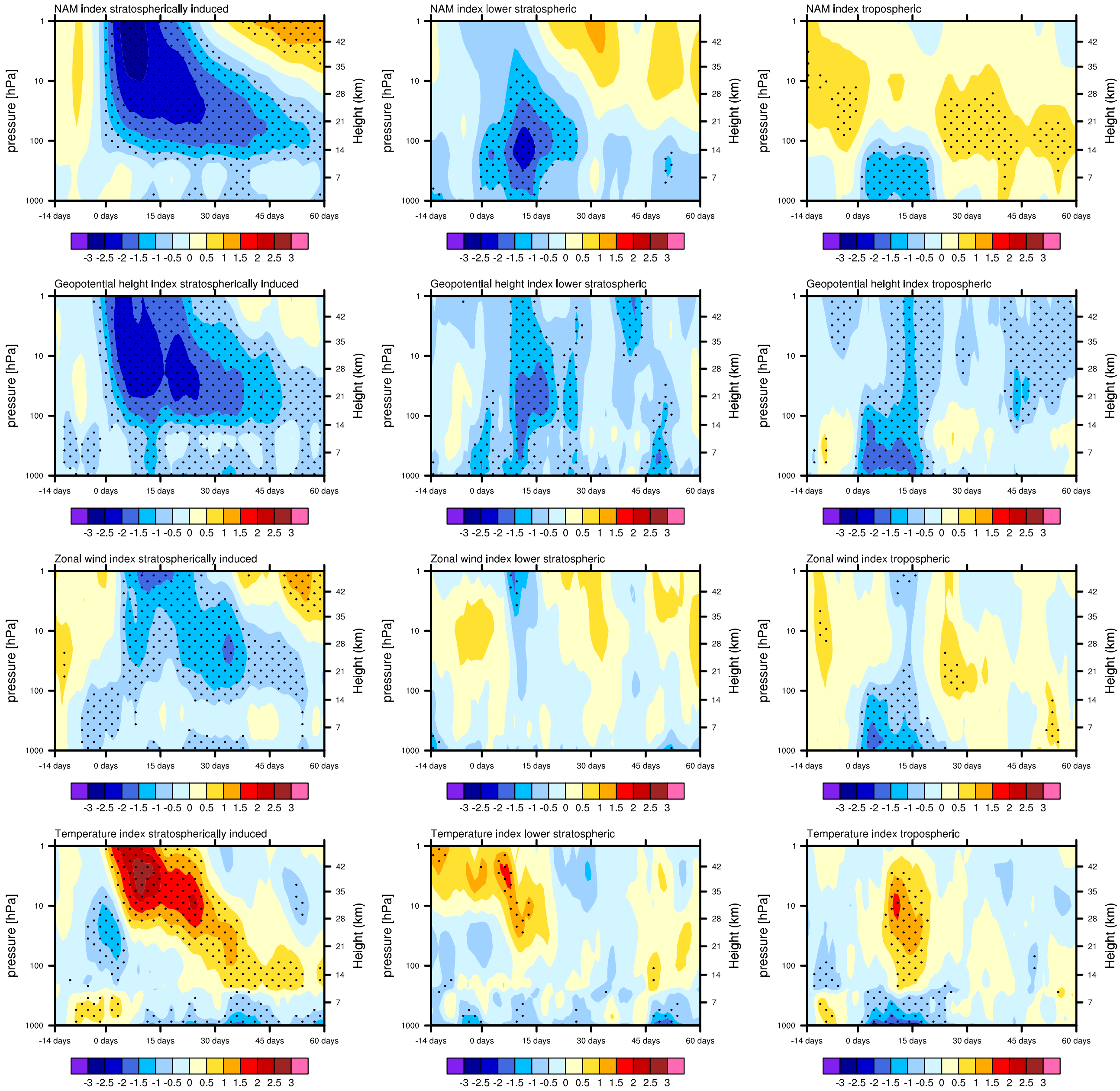

Figure 6. Time development of different indices for stratospherically induced (left column), lower stratospheric (mid column) and tropospheric (right column) cold spells: NAM index (first row), regional geopotential height index (second row), regional wind index (third row), and regional temperature index (fourth row). Stippling indicates areas where the anomalies exceed 2 standard deviations of natural variability.

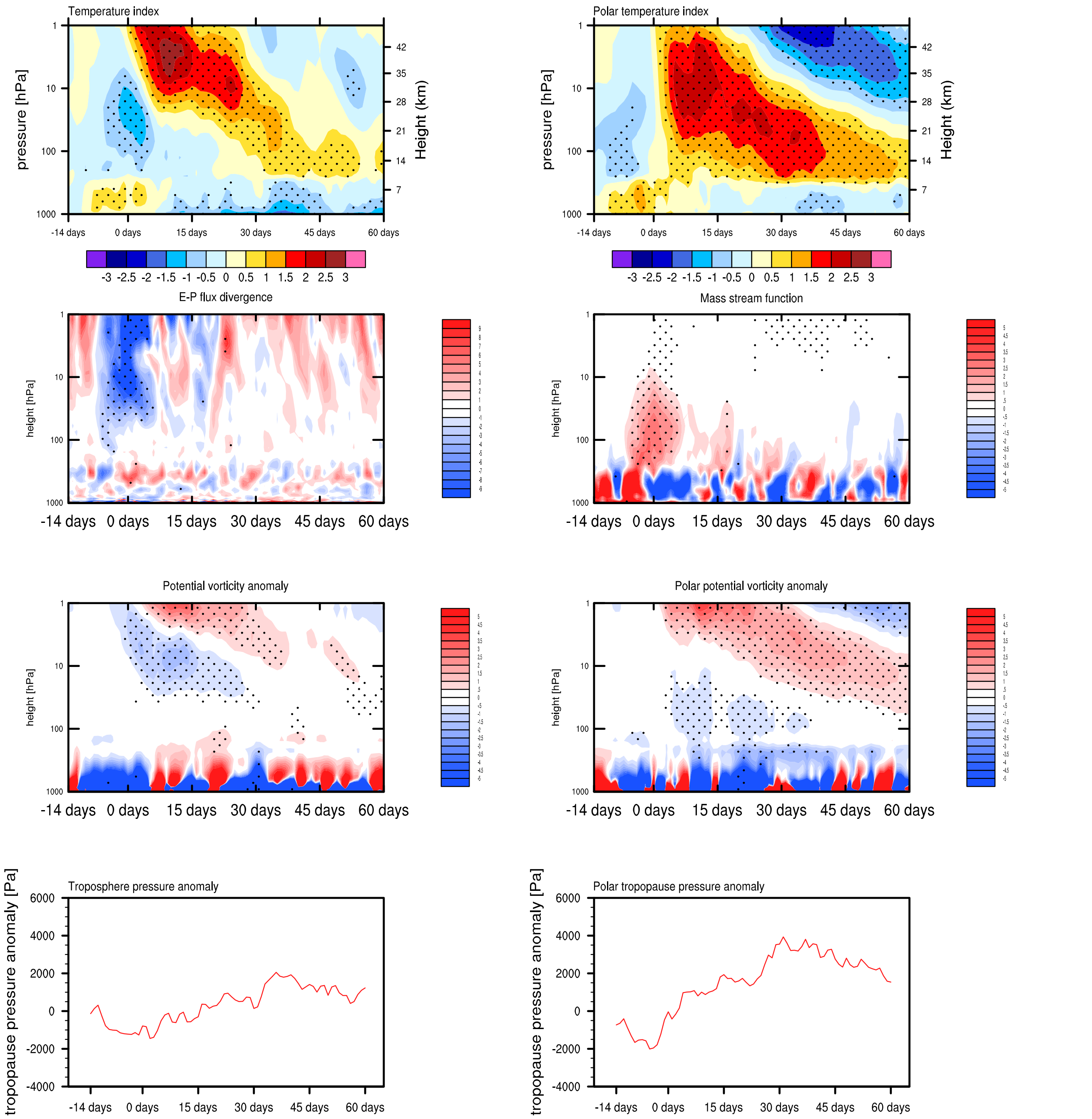

Figure 7. Time development of different diagnostics for stratospherically induced cold spells. First row: mid-latitudinal temperature anomalies (left panel), polar temperature anomalies (right panel). Second row: mid-latitudinal E-P flux divergence anomalies (left panel), mid-latitudinal residual circulation anomalies (right panel). Third row: mid-latitudinal potential vorticity anomalies (left panel), polar potential vorticity anomalies (right panel). Fourth row: mid-latitudinal tropopause height anomalies (left panel), polar tropopause height anomalies (right panel).

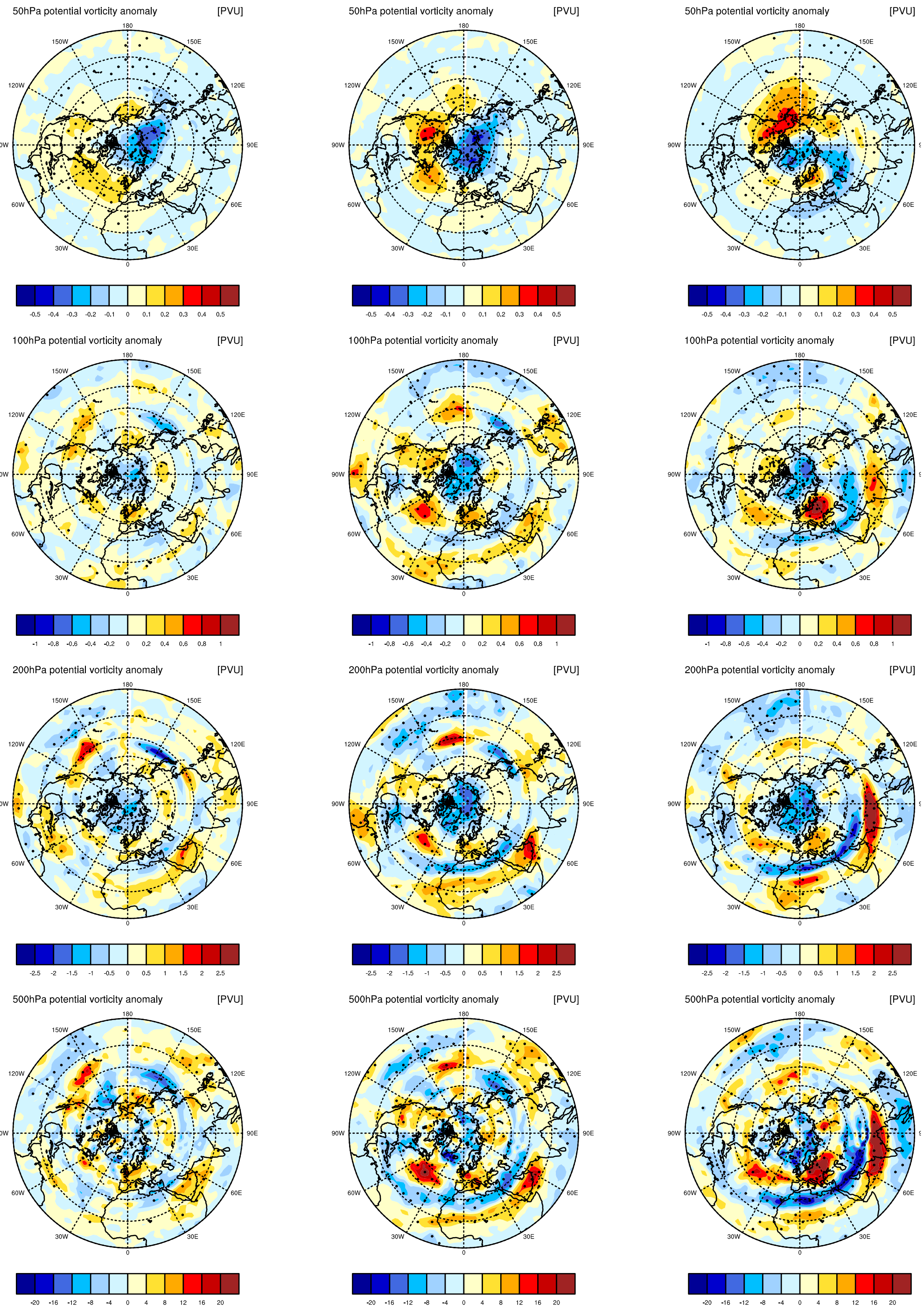

Figure 8. Time development of potential vorticity anomalies before and during the stratospherically induced cold spells. Left column: mean over days 30 to 15 before. Middle column: mean over day 15 to day 1 before. Right column: mean over day 1 to day 15 of the cold spells. Areas that exceed 2 standard deviations of natural variability are stippled.

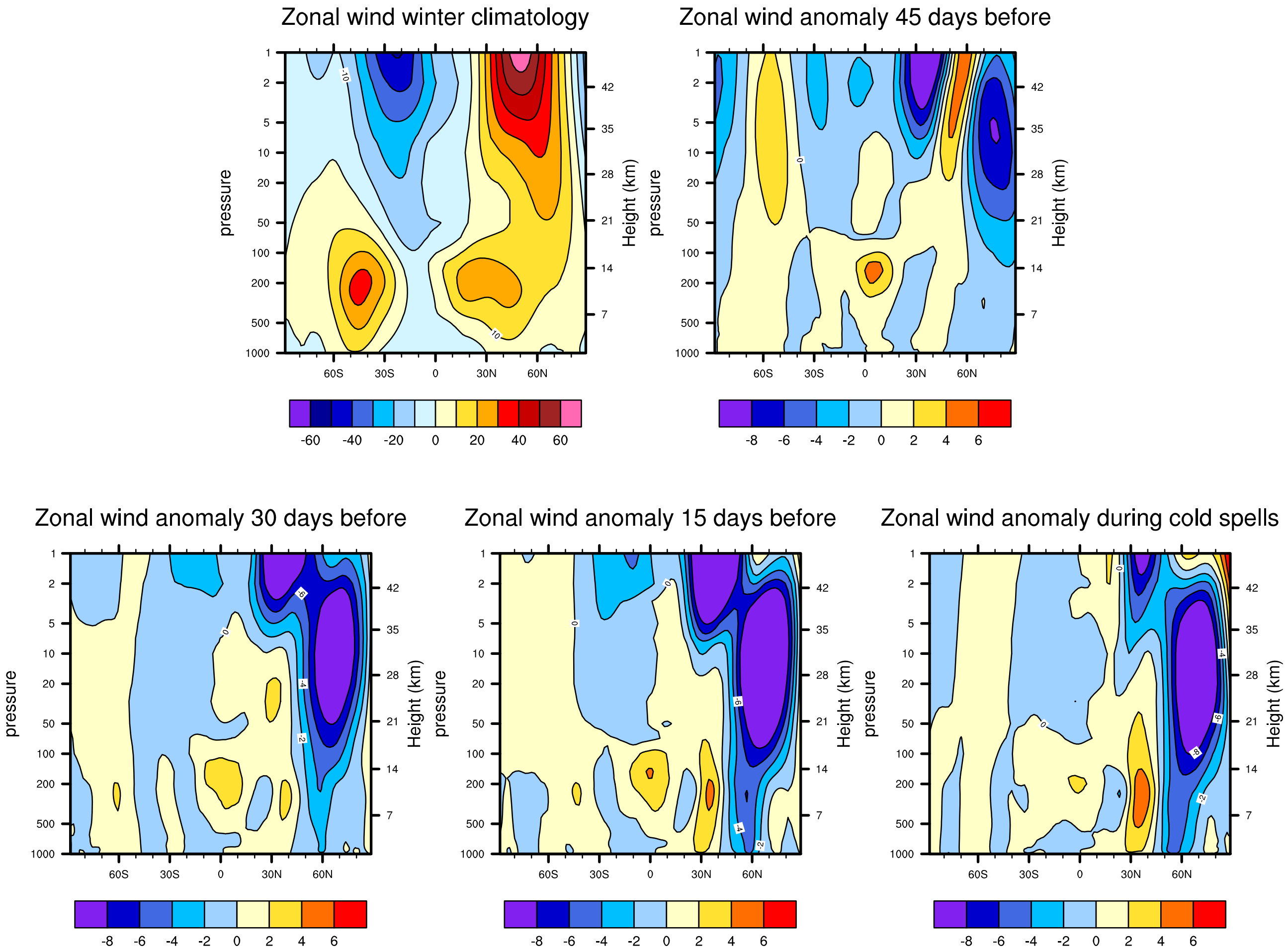

Figure 9. Upper row, left panel: winter (NDJFM) zonal-mean zonal wind climatology over the North-Atlantic sector (60 West to 20 East). Upper row, right panel: zonal-mean zonal wind anomalies for day 45 to day 30 before the cold spells. Lower row: zonal-mean zonal wind anomalies for day 30 to day 15 before (left panel), day 15 to day 1 before the cold spells (mid panel), and day 1 to day 15 during the cold spells (right panel).